ORIGINAL ARTICLE

CANCER COMMUNICATIONS
Open Access

N-acetyltransferase 10 promotes colon cancer progression by inhibiting ferroptosis through N4-acetylation and stabilization of ferroptosis suppressor protein 1 (FSP1) mRNA

Xiao Zheng[1,2,3] | Qi Wang[1,2,3] | You Zhou[1,2,3] | Dachuan Zhang[4] | Yiting Geng[2,5] | Wenwei Hu[2,5] | Changping Wu[1,2,5] | Yufang Shi[1,2,6,7] | Jingting Jiang[1,2,3,8]

[1]Department of Tumor Biological Treatment, the Third Affiliated Hospital of Soochow University, Changzhou, Jiangsu 213003, P. R. China

[2]Jiangsu Engineering Research Center for Tumor Immunotherapy, Changzhou, Jiangsu 213003, P. R. China

[3]Institute for Cell Therapy of Soochow University, Changzhou, Jiangsu 213003, P. R. China

[4]Department of Pathology, the Third Affiliated Hospital of Soochow University, Changzhou, Jiangsu 213003, P. R. China

[5]Department of Oncology, the Third Affiliated Hospital of Soochow University, Changzhou, Jiangsu 213003, P. R. China

[6]Institute for Translational Medicine of Soochow University, Suzhou, Jiangsu 215000, P. R. China

[7]CAS Key Laboratory of Tissue Microenvironment and Tumor, Shanghai Institute of Nutrition and Health, University of Chinese Academy of Sciences, Chinese Academy of Sciences, Shanghai 200031, P. R. China

[8]State Key Laboratory of Pharmaceutical Biotechnology, Nanjing University, Nanjing, Jiangsu 210023, P. R. China

Correspondence
Jingting Jiang, Department of Tumor Biological Treatment, the Third Affiliated Hospital of Soochow University, Changzhou, Jiangsu 213003, P. R. China.
Email: jiangjingting@suda.edu.cn

Abstract

Background: N-acetyltransferase 10 (*NAT10*) is the only enzyme known to mediate the N4-acetylcytidine (ac4C) modification of mRNA and is crucial for mRNA stability and translation efficiency. However, its role in cancer development and prognosis has not yet been explored. This study aimed to examine the possible role of *NAT10* in colon cancer.

Methods: The expression levels of *NAT10* were evaluated by immunohistochemical analyses with a colon cancer tissue microarray, and its prognostic value in patients was further analyzed. Quantitative real-time polymerase chain reaction (qRT-PCR) and Western blotting were performed to analyze *NAT10* expression in harvested colon cancer tissues and cell lines. Stable *NAT10*-knockdown and *NAT10*-overexpressing colon cancer cell lines were constructed using lentivirus. The biological functions of *NAT10* in colon cancer cell lines were analyzed in

Abbreviations: ac4C, N4-acetylcytidine; ANOVA, One-way analysis of variance; CCK-8, Cell Counting Kit-8; CRP, C-reaction protein; DMEM, Dulbecco's Modified Eagle Medium; EdU, 5-ethynyl-2′-deoxyuridine; *FSP1*, ferroptosis suppressor protein 1; GEO, Gene Expression Omnibus; GSH, glutathione; LDH, Lactate dehydrogenase; MDA, malondialdehyde; *NAT10*, N-acetyltransferase 10; qRT-PCR, Quantitative Realreal-time polymerase chain reaction; RIP, RNA immunoprecipitation; ROS, reactive oxygen species; *γ*H2AX, phosphorylated H2A.X variant histone.

vitro by Cell Counting Kit-8 (CCK-8), wound healing, Transwell, cell cycle, and ferroptosis assays. Xenograft models were used to analyze the effect of *NAT10* on the tumorigenesis and metastasis of colon cancer cells in vivo. Dot blotting, acetylated RNA immunoprecipitation-qPCR, and RNA stability analyses were performed to explore the mechanism by which *NAT10* functions in colon cancer progression.

Results: *NAT10* was upregulated in colon cancer tissues and various colon cancer cell lines. This increased *NAT10* expression was associated with shorter patient survival. Knockdown of *NAT10* in two colon cancer cell lines (HT-29 and LoVo) impaired the proliferation, migration, invasion, tumor formation and metastasis of these cells, whereas overexpression of *NAT10* promoted these abilities. Further analysis revealed that *NAT10* exerted a strong effect on the mRNA stability and expression of ferroptosis suppressor protein 1 (*FSP1*) in HT-29 and LoVo cells. In these cells, *FSP1* mRNA was found to be modified by ac4C acetylation, and this epigenetic modification was associated with the inhibition of ferroptosis.

Conclusions: Our study revealed that *NAT10* plays a critical role in colon cancer development by affecting *FSP1* mRNA stability and ferroptosis, suggesting that *NAT10* could be a novel prognostic and therapeutic target in colon cancer.

KEYWORDS

Colon cancer, N-acetyltransferase 10 (*NAT10*), N4-acetylcytidine (ac4C), Ferroptosis suppressor protein 1 (*FSP1*), Ferroptosis, mRNA stability, RNA acetylation

1 | BACKGROUND

Colon cancer remains a leading cause of cancer-related death worldwide, and 30%-50% of patients experience recurrence, metastasis, and even death within 5 years of treatment [1–4]. Although screening and treatment strategies for colon cancer have improved in recent years, the prognosis of advanced colon cancer remains poor largely due to a lack of understanding of the molecular mechanisms underlying its development [5–11].

Since the 1950s, evidence about chemical modifications of nucleosides in RNA, which extensively affect RNA structure, biogenesis, and function, has been increasing; thus our understanding of the complexity of RNA has been increasing [12]. N-acetyltransferase 10 (*NAT10*) is a lysine acetyltransferase that acetylates RNA [13, 14]. *NAT10* is found in the nucleolus and regulates telomerase activity, ribosomal RNA transcription, and cytokinesis [15–17]. A previous study reported that self-acetylated *NAT10* activated ribosomal RNA biogenesis, while *NAT10* was inhibited by Sirtuin 1-mediated deacetylation [17]. In addition, *NAT10* activates p53 via the acetylation of damaged DNA and stabilizes microtubules via the acetylation of α-tubulin [18]. Notably, *NAT10* has been associated with various cancers, such as breast cancer [16] and hepatocellular carcinoma [19]. The addition of N4-acetylcytidine (ac4C) is a conserved chemical RNA modification [20]. Several studies have shown that the addition of ac4C improved the fidelity or accuracy of protein translation [21–23]. Recent studies have also found that ac4C is widely present in oscillating sites of mRNA, where it helps to maintain mRNA stability and improve translation efficiency [24, 25]. It should be noted that ac4C acetylation, the first acetylation modification identified in mRNA, is associated with the occurrence and prognosis of various diseases [20, 26–29]. However, the precise role of *NAT10*-mediated ac4C acetylation in the progression and metastasis of colon cancer remains unclear.

Ferroptosis is involved in physiological processes and various diseases, such as cancer, and it is characterized by unique properties and recognition functions [30–33]. Unlike autophagy and apoptosis, ferroptosis is a form of cell death characterized by cytological changes, including reduced or absent mitochondrial crests, reactive oxygen species production, and membrane damage [34–36]. Although cancer cells are in a state of constant oxidative stress, the delicate balance between mercaptan and catalytic iron prevents iron sagging during cancer development [37–39]. However, the molecular mechanism underlying iron sagging has not yet been elucidated.

In this study, we evaluated the functional role of *NAT10* in colon cancer progression and analyzed its prognostic value for colon cancer patients. We further explored whether the regulation of ferroptosis is a critical mechanism by which *NAT10* functions in colon cancer and whether ferroptosis regulators are direct targets of ac4C acetylation.

2 | MATERIALS AND METHODS

2.1 | Patients and tissue samples

Samples of colon cancer tissues (International Classification of Diseases, 11th edition, code 2B90) and normal adjacent tissues were collected from patients undergoing surgical resection at the Third Affiliated Hospital of Soochow University (Changzhou, Jiangsu, China) between January 2014 and December 2017. The following patients were excluded: (1) those who received neoadjuvant chemotherapy or radiotherapy and (2) those who had other cancers. All the patients were classified according to the 8th edition of TNM staging system released by the Union for International Cancer Control and American Joint Committee on Cancer. Written informed consent was obtained from all the participants. Their clinicopathological characteristics are presented in Supplementary Table S1. The samples were frozen in liquid nitrogen and stored at $-80°C$ until use.

2.2 | Immunohistochemistry (IHC) of NAT10

IHC assays were performed to evaluate *NAT10* expression in human colon cancer tissues as well as adjacent normal tissues following a previously described protocol [40]. Briefly, a paraffin-embedded colon cancer tissue microarray (HColA180Su21, Shanghai Outdo Biotech Co. Ltd., Shanghai, China) was dried, dewaxed, and then rehydrated in gradient ethanol solutions. After the sections were immersed, they were rinsed phosphate-buffered saline solution (PBS, C0221A, Beyotime, Shanghai, China) and blocked with bovine serum albumin (1 mg/mL, ST2254, Beyotime) in PBS. The sections were incubated with a rabbit anti-human *NAT10* monoclonal antibody (1:200, ab194297, Abcam, Cambridge, MA, USA) at 4°C overnight. The sections were washed the next morning and incubated with a secondary antibody (ab205719, Abcam) for 30 min at 37°C. The dehydrated sections were then cleared and mounted; diaminobenzene was used as the chromogen, and hematoxylin was used as the nuclear counterstain. The immunostaining intensity of *NAT10* was measured based on the previously described H-score method [40].

Two pathologists who were blinded to the patients' clinical data made the diagnosis according to the 8th edition of the Union for International Cancer Control and American Joint Committee on Cancer TNM Staging Manual. According to the immunoreactivity scores, the colon cancer patients were divided into two groups: low expression (H-score ≤ 100) and high expression (H-score > 100).

2.3 | RNA extraction and quantitative real-time polymerase chain reaction (qRT-PCR) analysis

Following a previously described protocol [40], RNA extraction and qRT-PCR were performed using the ABI vii7 system (Applied Biosystems, Foster City, CA, USA). The reaction conditions were as follows: denaturing at 95°C for 30 s, followed by 40 cycles of annealing at 60°C for 30 s and elongation at 72°C for 30 s. The SYBR green reagent (4472908, Thermo Fisher, Waltham, MA, USA) was used, and human glyceraldehyde-3-phosphate dehydrogenase (*GAPDH*) was chosen as the housekeeping gene. The following primers were synthesized and used: human *NAT10* forward primer: 5'-TCACTCCCCGGAAGGACCTG-3', and reverse primer: 5'-AGCCTGGGGGTCAAGCCATA-3'; ferroptosis suppressor protein 1 (*FSP1*) forward: 5'-CAAGTGGCCCTGGCTGACAA-3', and *FSP1* reverse: 5'-TGGCCACCTCTGTGCCTTTG-3'; *GAPDH* forward: 5'-TGACTTCAACAGCGACACCCA-3', and *GAPDH* reverse: 5'-CACCCTGTTGCTGTAGCCAAA-3'. Relative gene expression was normalized to *GAPDH* mRNA expression and analyzed using the comparative CT method ($\Delta\Delta$CT).

2.4 | Western blotting analysis

Western blotting analysis was performed as previously described [40]. Anti-*NAT10* (1:1000, ab194297, Abcam) and HRP-labeled anti-*GAPDH* antibodies (1:5000, KC5G4, Kancheng Biotechnology, Shanghai, China) were used. A chemiluminescence detection kit from Thermo Fisher was used to visualize the immunoreaction. A video documentation system (Gel Doc 2000, Bio-Rad, Hercules, CA, USA) was used to quantify the band densities.

2.5 | Total ac4C quantification

Total RNA from each sample was harvested, and the quantification of the ac4C levels was performed by using a Total ac4C acetylation Quantification kit (GK-4040, Colorimetric, Genelily Biotech, Shanghai, China) according to the manufacturer's instructions.

2.6 | Ac4C dot blotting

Total RNA from each sample was heated to 75°C for 5 min, cooled for 1 min, and loaded onto Amersham Hybond-N+ membranes (0.45 μm, YA1760, Solarbio, Beijing, China). The membranes were crosslinked, blocked, and incubated with an anti-ac4C antibody (1:2000, ab252215, Abcam) at 4°C overnight. The membranes were then washed and probed with an HRP-conjugated secondary anti-rabbit IgG at 25°C for 1 h. We then washed the membranes three times and visualized the proteins of interest with the Chemiluminescent HRP substrate (WBKLS0500, Millipore, Billerica, MA, USA). After exposure, the membranes were stained with methylene blue staining buffer with gentle shaking for 30 min and then washed with ribonuclease-free water. Then, the input RNA was scanned to determine its total content.

2.7 | Cell lines and cell culture

The human colon cancer cell lines (HT-29, HCT-116, SW480, SW620, LoVo, SW48, DLD-1, Caco-2, HCT-15) and a normal human colon mucosal epithelial cell line NCM460 were purchased from the Chinese Academy of Sciences, Shanghai Institutes for Biological Sciences (Shanghai, China) and verified by short tandem repeat genotyping. Dulbecco's Modified Eagle Medium (DMEM, 11960077, Gibco, Grand Island, NY, USA) supplemented with 10% fetal bovine serum (10099141, Gibco) was used to maintain all the cell lines under standard conditions (5% CO_2, 37°C). For the ferroptosis inhibition groups, ferrostatin-1 (2 μmol/L, HY-100579, MedChemExpress, Princeton, NJ, USA) was added to the complete culture medium.

2.8 | Construction of stable NAT10-knockdown and NAT10-overexpressing colon cancer cell lines

To construct stable *NAT10*-knockdown colon cancer cell lines (HT-29 and LoVo), short hairpin RNA (shRNA) specifically targeting *NAT10* was designed by the Invitrogen online tool (https://rnaidesigner.thermofisher.com/rnaiexpress/) and cloned into the lentiviral pLVX-sh1 vector. For the construction of stable *NAT10*-overexpressing colon cancer cell lines (SW-480 and DLD-1), the human *NAT10*-coding sequence (NM_024662.3) was purchased from Generalbiol Biotech (Hefei, Anhui, China) and cloned into the lentiviral pLVX-IRES-puro vector. The shRNA sequences and *NAT10*-coding sequences are pre-sented in Supplementary Table S2. Lentiviruses carrying *NAT10* shRNA or the *NAT10*-coding sequences were constructed by Genelily Biotech Co., Ltd. The colon cancer HT29 and SW480 cell lines were infected with lentivirus in 6-well plate following the manufacturer's instructions. The medium was replaced with complete medium the next day. Stably infected colon cancer cells were selected by incubation with 2 μg/mL puromycin for two weeks. The efficiency of *NAT10* knockdown or overexpression was examined by qRT-PCR and Western blotting.

2.9 | Cell proliferation assay

Cell proliferation was measured by Cell Counting Kit-8 (CCK-8, Dojindo, Tokyo, Japan) assays as previously described [40]. Briefly, cells were seeded in a 96-well plate at a density of 1×10^3 cells/well and cultured for the indicated time points (0, 24, 48, 72 h). After incubation with 10 μL of CCK-8 reagent for 1 h, the absorbance at 450 nm was measured.

2.10 | Colony formation assay

Colon cancer cells were cultivated in 6-well plates at a concentration of 1×10^4 cells per well. A 10-day culture was terminated by fixation with 4% paraformaldehyde and staining with 1% crystal violet. The colony forming units within each well were subsequently photographed and recorded by an Olympus CX53 microscope (Tokyo, Japan).

2.11 | Cell cycle analysis

Cell cycle distribution was assessed by propidium iodide (PI, A601112, Sango Biotech, Shanghai, China) staining, followed by flow cytometry analysis. Colon cancer cells were harvested, washed, and resuspended in DMEM at a concentration of 1×10^5 cells/tube. Then, the cells were fixed and incubated with RNase A (BioLegend, San Diego, CA, USA) and PI solution. A flow cytometer (FACS Canto^{TM} II, BD Biosciences, Franklin Lakes, NJ, USA) was used to generate DNA histograms to assess the cell cycle distribution.

2.12 | Cell migration assay

Cell migration was assessed using a wound healing assay as previously described [40]. Briefly, a 200 μL pipette tip was used to scratch the cell monolayer, and the wound width was captured after 0 and 24 h by an Olympus CX53

microscope with a digital camera. The migration distance was analyzed using ImageJ software (National Institutes of Health, Bethesda, MD, USA).

2.13 | Cell invasion assay

Cell invasion was examined using Matrigel (BD Bioscience)-coated Transwell chambers (8 μm pore size, BD Bioscience) as previously described [40]. Briefly, colon cancer cells in a total of 200 mL serum-free medium were seeded in the Matrigel-coated upper chamber. The chambers were fixed in 4% paraformaldehyde for 10 min and stained with crystal violet after 24 h. Images were captured by an Olympus CX53 microscope with a digital camera, and the number of metastatic cells was counted using ImageJ software.

2.14 | Tumor xenografts

BALB/c nude mice (5 weeks old, male) were purchased from the Shanghai Laboratory Animal Center (Shanghai, China). For the tumorigenesis assay, knockdown negative control (shNC) HT-29 cells, NAT10-knockdown (shNAT10) HT-29 cells, overexpression control (oeNC) SW480 cells and NAT10-overexpression (oeNAT10) SW480 cells were subcutaneously injected into the backs of nude mice. In the ferroptosis inhibition groups, ferrostatin-1 (1 mg/kg) was injected via the tail vein every five days. The tumor size was measured every five days, and the tumor volume was calculated as follows: tumor volume = (length × width^2) / 2. For the EdU incorporation assay, the mice were intraperitoneally injected with EdU (100 mg/kg, Beyotime) 24 h before being euthanized. After 30 days, the mice were euthanized by CO_2 inhalation, and the tumors were removed, photographed, weighed, and fixed for EdU staining according to the manufacturer's protocol.

For the lung metastasis experiment, HT29 (shNC and shNAT10) and SW480 (oeNC and oeNAT10) cells were injected into the tail veins of nude mice to assess their metastatic ability. In the ferroptosis inhibition groups, ferrostatin-1 (1 mg/kg) was injected via the tail vein every five days. After 30 days, the mice were euthanized by CO_2 inhalation. The lungs were then excised and fixed for H&E staining and IHC analysis. The number of lung tumor metastases was calculated.

2.15 | RNA-sequencing (RNA-seq)

RNA-seq was conducted to screen the potential NAT10-regulated mRNAs following a previously described protocol [40]. We used HiSeq RNA-Seq using a HiSeq 4000 (Illumina, San Diego, CA, USA) for total RNA-seq, and HISAT2 (http://daehwankimlab.github.io/hisat2/) was used to map the transcriptome reads to the reference genome (hg19). Next, gene expression levels were quantified using the Ballgown package.

2.16 | Acetylation site prediction

The conserved acetylation sites in the FSP1 messenger RNA-coding sequences were predicted by PACES tools (http://rnanut.net/paces/) with a specificity of 99%.

2.17 | ac4C RNA immunoprecipitation (RIP) assay and qRT-PCR

ac4C-RIP was performed using an RNA immunoprecipitation kit (GK-5044, Genelily Biotech) according to the manufacturer's instructions. Briefly, cells were lysed with 1 mL RIP lysis buffer for 10 min, and then 100 μL of the lysates were stored at −80°C. An anti-ac4C antibody (1:50, ab252215, Abcam) or normal rabbit IgG (1:50, 2729S, Cell Signaling Technology, Beverly, MA, USA) was mixed with protein A/G beads at 4°C for 2 h and then incubated with 450 μL of the lysate at 4°C for 2 h. After washing the beads with buffer, the RNA was extracted, and then qRT-PCR was performed as previously described.

2.18 | Gene Expression Omnibus (GEO) database analysis

The FSP1 expression in colon cancer tissues was analyzed with the GEO dataset (GSE31782, https://www.ncbi.nlm.nih.gov/geo/).

2.19 | RNA stability assay

HT-29 cells were treated with actinomycin D (5 μg/mL, HY-17559, MedChemExpress) for 0, 1, 3, and 6 h in 6-well plates. The FSP1 mRNA half-life was estimated by linear regression analysis of total RNA collected using the method described above for quantitative real-time PCR analysis.

2.20 | Luciferase report assay

We first constructed two luciferase reporter plasmids by inserting partial FSP1 mRNA sequences with wild-type or C132A-mutated ac4C sites. For luciferase assays, colon cancer cells were seeded in 24-well plates at a concentration of

1×10^5 cells/well. The cells were transfected with the plasmid with Lipofectamine 3000 (L3000015, Thermo Fisher). After transfection for 24 h, we measured the activity of luciferase in the harvested cells using the Dual-Luciferase Reporter Assay System (Promega, E1910, San Luis Obispo, CA, USA). The relative luciferase activity was normalized to the Renilla luciferase activity.

2.21 | Ferroptosis assay

It is well known that lipid-reactive oxygen species (ROS) accumulation, lipid peroxidation, glutathione (GSH) depletion, and iron accumulation are critical indicators of ferroptosis. Therefore, we measured the levels of intracellular ROS with the 2'-7'dichlorofluorescin diacetate (DCFH-DA) dye (S0033S, Beyotime) according to the manufacturer's instructions. The level of GSH was analyzed using a Glutathione Assay Kit (CS0260, Sigma-Aldrich, CA, USA) according to the instructions. The level of malondialdehyde (MDA) was analyzed with a TBA method Kit (A003, Nanjing Jiancheng, Nanjing, Jiangsu, China) following the manufacturer's instructions. The cellular concentration of iron was measured by an Iron Assay Kit (ab83366, Abcam) according to the manufacturer's instructions. The lactate dehydrogenase (LDH) activity in serum was measured with an LDH Activity Kit (BC0680, Solarbio). The serum levels of C-reaction protein (CRP) were measured with a CRP ELISA kit (EK1316, Boxter, Wuhan, Hubei, China). The level of phosphorylated H2A.X variant histone (γH2AX) was measured by a phospho-gamma H2A.X (S139) ELISA Kit (ab279816, Abcam).

2.22 | Transmission electron microscopy (TEM)

The morphological characteristics of ferroptosis in colon cancer cells were analyzed by TEM. Briefly, a total of 2×10^4 cells were seeded onto a chambered cover glass (Thermo Fisher). TEM images were captured by a Hitachi HT-7700 transmission electron microscope (Hitachinaka, Ibaraki, Japan).

2.23 | Statistical analysis

The data are expressed as the mean ± standard deviation. The experiments were repeated three times, and all the statistical analyses were conducted using GraphPad Prism 9.0 (GraphPad Software, Inc., San Diego, CA, USA). Student's t test, one-way analysis of variance (ANOVA), and two-factor ANOVA were used to compare differences between and among groups. For all the statistical tests, $P < 0.05$ (bilateral) was considered to indicate statistical significance.

3 | RESULTS

3.1 | NAT10 was upregulated in colon cancer cells and was associated with a short survival

To understand the potential role of *NAT10* in colon cancer, we performed IHC analyses with a tissue microarray that included tumor tissues and paired adjacent tissues from 90 patients. Clinicopathological characteristics of these patients are summarized in Table 1. The IHC results showed that the *NAT10* protein levels were predominantly localized in the nuclei of colon cancer cells (Figure 1A) and were significantly higher than those in adjacent normal tissues (Figure 1B). The overall survival of patients with low *NAT10* expression seemed to be longer than that of patients with high *NAT10* expression ($P = 0.026$, hazard ratio = 0.48, 95% confidence interval = 0.21-1.09, Figure 1C). Moreover, we performed a chi-square test to evaluate the associations between *NAT10* expression and clinicopathological characteristics. The results showed that the expression of *NAT10* was associated with lymph node metastasis and T stage (Table 1). We further evaluated the *NAT10* mRNA and protein levels in 20 paired fresh colon cancer tissues and adjacent tissues. The results showed that the *NAT10* mRNA (Figure 1D) and protein levels (Figure 1E) were significantly higher in colon cancer tissues than in the paired adjacent tissues. Consistently, the total ac4C acetylation of RNA, which was quantified by the Colorimetric Kit (Figure 1F) and dot blotting (Figure 1G), was also significantly increased in the colon cancer tissues. Moreover, the *NAT10* mRNA (Figure 1H) and protein levels (Figure 1I) in cultured colon cancer cell lines HT-29, HCT-116, SW480, SW620, LoVo, SW48, DLD-1, Caco-2, and HCT-15 were significantly higher than those in a normal human colon mucosal epithelial cell line NCM460. Collectively, these results suggest that *NAT10* expression is upregulated in colon cancer and that this upregulated *NAT10* expression is associated with a poor prognosis.

3.2 | NAT10 promoted the proliferation of colon cancer cells both in vitro and in vivo

To evaluate the functional role of *NAT10* in colon cancer, we established several stable *NAT10*-knockdown cell lines (HT-29 and LoVo cell lines) and *NAT10*-overexpressing
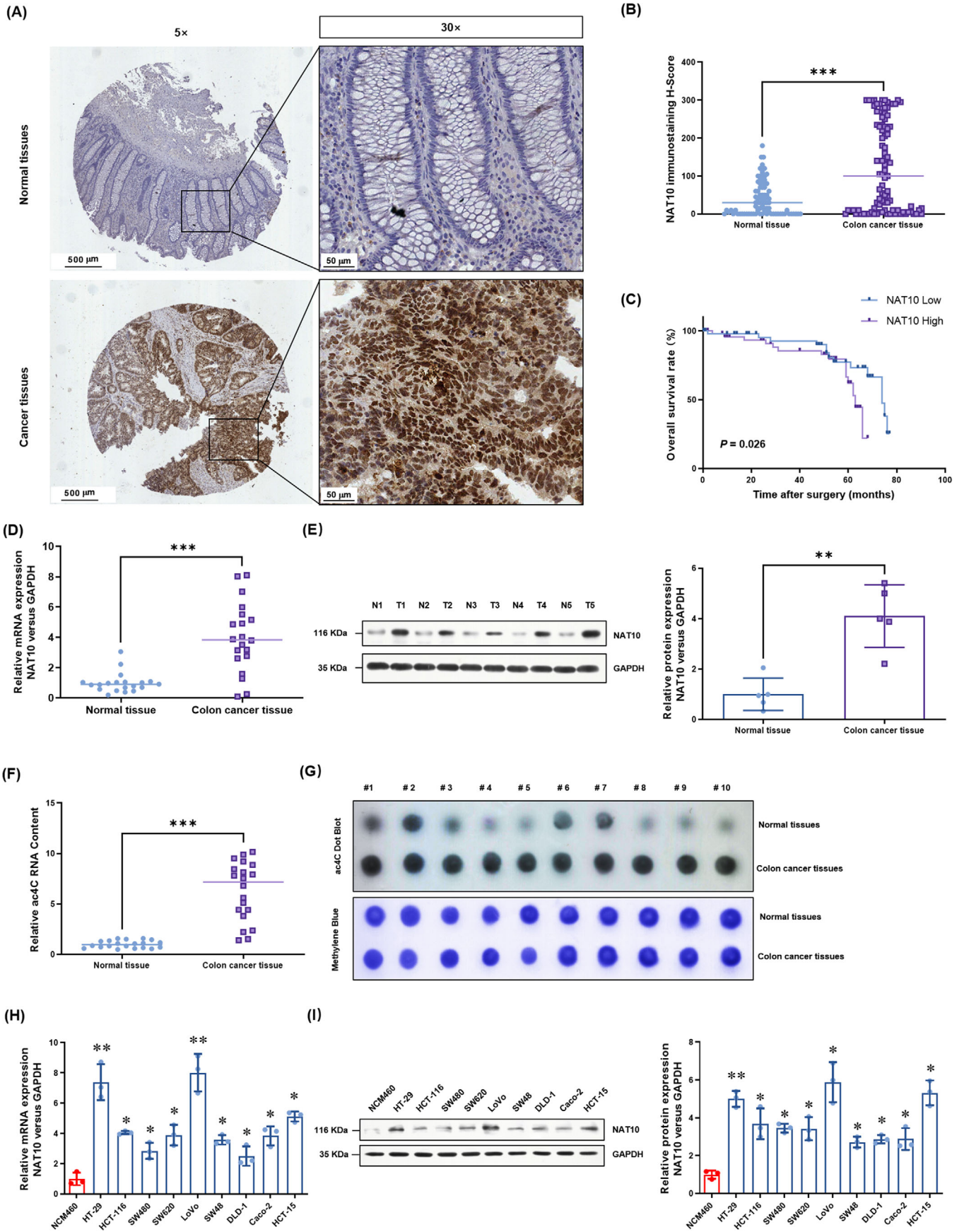
(A)

(B)

(C)

(D)

(E)

(F)

(G)

(H)

(I)

TABLE 1 Associations between *NAT10* expression and clinicopathological characteristics of 90 patients with colon cancer

Clinical parameter	Total [cases (%)]	NAT10 expression level [cases (%)]		χ^2	*P*
		Low	High		
Total	90	43 (47.8)	47 (52.2)		
Gender				0.156	0.693
Female	48 (53.3)	22 (45.8)	26 (54.2)		
Male	42 (46.7)	21 (50.0)	21(50.0)		
Age (years)				0.062	0.803
<65	41 (45.6)	19 (46.3)	22 (53.7)		
≥65	49 (54.4)	24 (49.0)	25 (51.0)		
Tumor size (cm)				0.556	0.456
≤5	35 (38.9)	15 (42.9)	20 (57.1)		
>5	55 (61.1)	28 (50.9)	27 (49.1)		
Pathological stage				0.569	0.451
I+II	58 (64.4)	26 (44.8)	32 (55.2)		
III	32 (35.6)	17 (53.1)	15 (46.9)		
Lymph node metastasis				2.392	**0.039**
Negative	57 (63.3)	26 (45.6)	31 (54.4)		
Positive	33 (36.7)	7 (21.2)	26 (78.8)		
T stage				2.258	**0.042**
T1-T2	39 (43.3)	26 (66.7)	13 (33.3)		
T3-T4	51 (56.7)	17 (33.3)	34 (66.7)		
N stage				0.584	0.445
N0-N1	56 (62.2)	25 (44.6)	31 (55.3)		
N2-N3	34 (37.8)	18 (52.9)	16 (47.1)		
M stage				1.637	0.201
M0	85 (94.4)	42 (49.4)	43 (50.6)		
M1	5 (5.6)	1 (20.0)	4 (80.0)		
TNM stage				3.110	0.375
I	9 (10.0)	3 (33.3)	6 (66.7)		
II	46 (51.1)	25 (54.3)	21 (45.7)		
III	30 (33.3)	14 (46.7)	16 (53.3)		
IV	5 (5.6)	1 (20.0)	4 (80.0)		

cell lines (SW480 and DLD-1 cell lines) via the lentivirus method. The real-time PCR results showed that the mRNA level of *NAT10* was significantly decreased in HT-29 and LoVo cells after *NAT10* knockdown (Figure 2A), and the decreased *NAT10* protein levels in these cells were then verified using Western blotting (Figure 2B). CCK-8 assay

results showed that cell proliferation was significantly suppressed after *NAT10* knockdown (Figure 2C). The numbers of colonies formed by *NAT10*-knockdown colon cancer cells were significantly lower than those formed by vector control cells (Figure 2D). Cell cycle analysis also showed that *NAT10* knockdown caused significant cell cycle arrest,

FIGURE 1 *NAT10* is upregulated in colon cancer and upregulated *NAT10* is associated with a poor prognosis. (A) Representative images and (B) quantitative analysis of IHC staining of *NAT10* expression showed the localization of *NAT10* in the nuclei of cancer cells and that *NAT10* is expressed at higher levels in tumor tissues (*n* = 90). (C) Overall survival of patients with low *NAT10* expression was significantly better than that of patients with high *NAT10* expression. (D) The mRNA and (E) protein levels of *NAT10* in fresh colon cancer tissues were higher than those in paired adjacent tissues (*n* = 20). (F) Colorimetric assay and (G) dot blotting show that the total ac4C levels in acetylated RNA in 10 fresh colon cancer tissues were higher than those in paired adjacent tissues. (H) *NAT10* mRNA and (I) protein levels are higher in cultured colon cancer cell lines than in the normal colon NCM460 cell line (*n* = 3). *$P < 0.05$, **$P < 0.01$, and ***$P < 0.001$. Abbreviations: KDa, kilodalton; *NAT10*, N-acetyltransferase 10; *GAPDH*, glyceraldehyde-3-phosphate dehydrogenase; ac4C, N4-acetylcytidine.
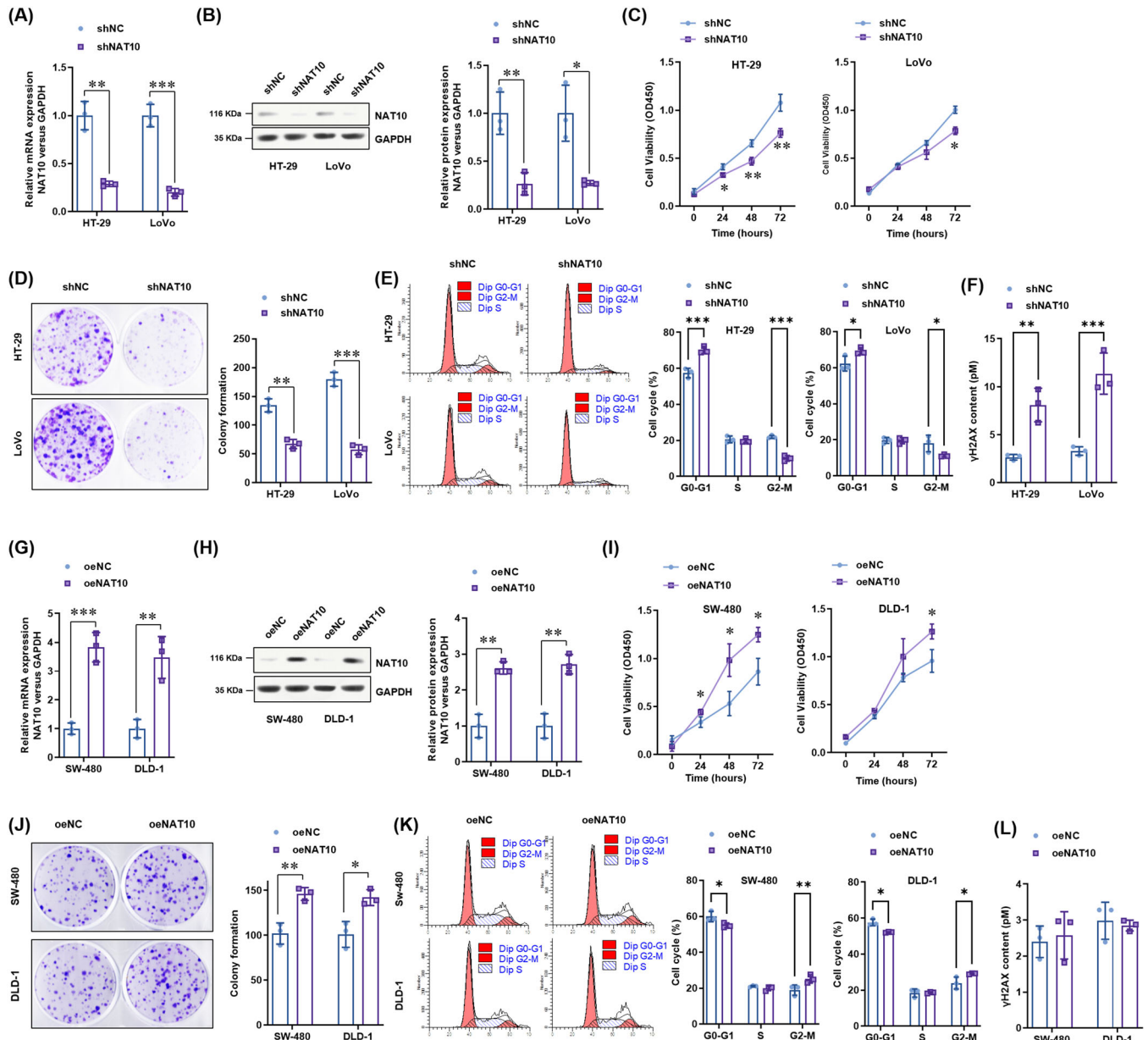
FIGURE 2 *NAT10* promotes the proliferation of colon cancer cells in vitro. (A) Knockdown of *NAT10* mRNA and (B) protein levels were confirmed by real-time PCR and Western blotting analysis ($n = 3$). (C-D) *NAT10* knockdown impaired cell proliferation as shown by CCK-8 assay (C) and colony formation assay (D) ($n = 3$). (E) The inhibitory effect of *NAT10* knockdown on the cell cycle progression of colon cancer cells was analyzed by flow cytometry. The Dip G0-G1, Dip S and Dip G2-M populations were analyzed and are presented ($n = 3$). (F) *NAT10* knockdown-induced DNA damage (γH2AX level) was analyzed by ELISA ($n = 3$). (G-H) The levels of *NAT10* mRNA (G) and protein (H) overexpression were confirmed by real-time PCR and Western blotting analysis ($n = 3$). (I-J) The promotion of cell proliferation by *NAT10* overexpression was analyzed by CCK-8 assay (I) and colony formation assay (J) ($n = 3$). (K) The effect of *NAT10* overexpression on the cell cycle progression of colon cancer cells was analyzed by flow cytometry. The Dip G0-G1, Dip S and Dip G2-M populations were analyzed and are presented ($n = 3$). (L) The effect of *NAT10* knockdown on the DNA damage (gH2AX level) of colon cancer cells was analyzed by ELISA ($n = 3$). *$P < 0.05$, **$P < 0.01$, and ***$P < 0.001$. Abbreviations: shNC, knockdown negative control, sh*NAT10*, *NAT10* knockdown; oeNC, overexpression control; oe*NAT10*, *NAT10* overexpression; KDa, kilodalton; *NAT10*, N-acetyltransferase 10; *GAPDH*, glyceraldehyde-3-phosphate dehydrogenase.

with an increased cell population in the G0-G1 phase and a decreased cell population in the G2-M phase (Figure 2E). DNA damage, as indicated by the level of γH2AX, was consistently observed after *NAT10* knockdown (Figure 2F).

Next, we explored the oncogenic role of *NAT10* in two colon cancer cell lines with comparably low *NAT10* expression (SW480 and DLD-1 cell lines). The *NAT10* mRNA and protein overexpression efficiency was confirmed using real-time PCR (Figure 2G) and Western blotting analysis (Figure 2H). The results showed that cell proliferation, as indicated by the CCK-8 assay (Figure 2I) and colony formation assay (Figure 2J), was significantly enhanced by *NAT10* overexpression. Cell cycle analysis further showed that *NAT10* could promote colon cancer cell progression from the G0/G1 phase to the G2-M phase, thus promoting cell proliferation (Figure 2K). However, *NAT10* did not affect the level of γH2AX (Figure 2L). These results suggest that *NAT10* promotes the proliferation of colon cancer cells in vitro.

To study whether *NAT10* promotes the proliferation of colon cancer cells in vivo, subcutaneous transplantation tumor models in nude mice were established using stable *NAT10*-knockdown HT-29 cells and stable *NAT10*-overexpressing SW480 cells. The results showed that *NAT10* knockdown significantly decreased the growth (Figure 3A-B) and weight (Figure 3C) of tumors derived from HT-29 cells. In contrast, *NAT10* overexpression significantly enhanced the growth (Figure 3A and 3D) and weight (Figure 3E) of tumors derived from SW480 cells. Consistently, the EdU staining in the tumors showed that *NAT10* knockdown significantly reduced the numbers of EdU-positive cells, whereas *NAT10* overexpression significantly increased the numbers of EdU-positive cells (Figure 3F). Altogether, these results demonstrate that *NAT10* promoted the proliferation of colon cancer cells both in vitro and in vivo.

3.3 | *NAT10* promoted the metastasis of colon cancer cells both in vitro and in vivo

The effect of *NAT10* on the metastasis of colon cancer cells was evaluated using wound healing and invasion assays. According to the results, *NAT10* knockdown significantly inhibited the migration of HT-29 and LoVo cells (Figure 4A) and decreased the number of invasive cells (Figure 4B). Consistently, the role of *NAT10* overexpression in promoting the migration (Figure 4C) and invasion (Figure 4D) of SW480 and DLD-1 cells was observed.

Next, we explored whether *NAT10* promotes the metastasis of colon cancer cells in vivo. Similar to the changes in the subcutaneous transplantation tumor model, *NAT10* knockdown significantly decreased the number of lung metastatic lesions generated by HT-29 cells, whereas *NAT10* overexpression increased the number of lung metastatic lesions generated by SW480 cells (Figure 4E). Moreover, histopathological diagnosis (H&E staining) further confirmed the decreased numbers of metastatic lesions in the *NAT10* knockdown group and increased numbers of metastatic lesions in the *NAT10* overexpression group (Figure 4F). Ki67 staining showed proliferation in the resected lung tissues, which also suggested that *NAT10* knockdown impaired the proliferation in lung metastasis lesions derived from HT-29 cells, whereas *NAT10* overexpression promoted the proliferation in those derived from SW-480 cells (Figure 4F). Overall, these results suggest that *NAT10* promotes the metastatic ability of colon cancer cells both in vitro and in vivo.

3.4 | *NAT10* improved the mRNA stability of *FSP1* and enhanced its expression in colon cancer cells

To further explore the underlying mechanisms by which *NAT10* promotes the proliferation and metastasis of colon cancer cells, a transcriptomic comparison was carried out to analyze the dysregulated genes between *NAT10*-knockdown and vector control HT-29 cells. A heatmap of the transcriptome (Figure 5A) showed that *FSP1*, a glutathione-independent ferroptosis suppressor, was mostly deregulated in *NAT10*-knockdown HT-29 cells. The decreased level of *FSP1* expression in *NAT10*-knockdown HT-29 and LoVo cells was verified using real-time PCR analysis (Figure 5B) and Western blotting (Figure 5C). Elevated *FSP1* levels were observed in *NAT10*-overexpressing SW-480 and DLD-1 cells by real-time PCR (Figure 5B) and Western blotting analysis (Figure 5C). In addition, a highly conserved acetylation site (Figure 5D) was predicted by PACES tools. The ac4C RIP-PCR results showed that the level of ac4C-acetylated *FSP1* mRNA was consistently decreased in *NAT10*-knockdown HT-29 and LoVo cells (Figure 5E) and increased in *NAT10*-overexpressing SW-480 and DLD-1 cells (Figure 5E). To understand the expression of *FSP1* in colon cancer tumor tissues, we queried the GEO dataset (GSE31782). The results confirmed the lower expression of *FSP1* in colon cancer tissues than in adjacent normal tissues (Figure 5F). Interestingly, a positive correlation was observed between the expression of *NAT10* and *FSP1* in colon cancer tissues (Figure 5G). The mRNA stability of *FSP1* was significantly reduced by *NAT10* knockdown (Figure 5H). To confirm that *NAT10*-mediated ac4C modification affected *FSP1* mRNA stability, we constructed recombinant luciferase reporter plasmids by inserting partial *FSP1* mRNA sequences with wild-type or C132A-mutated ac4C sites (Figure 5I). The results
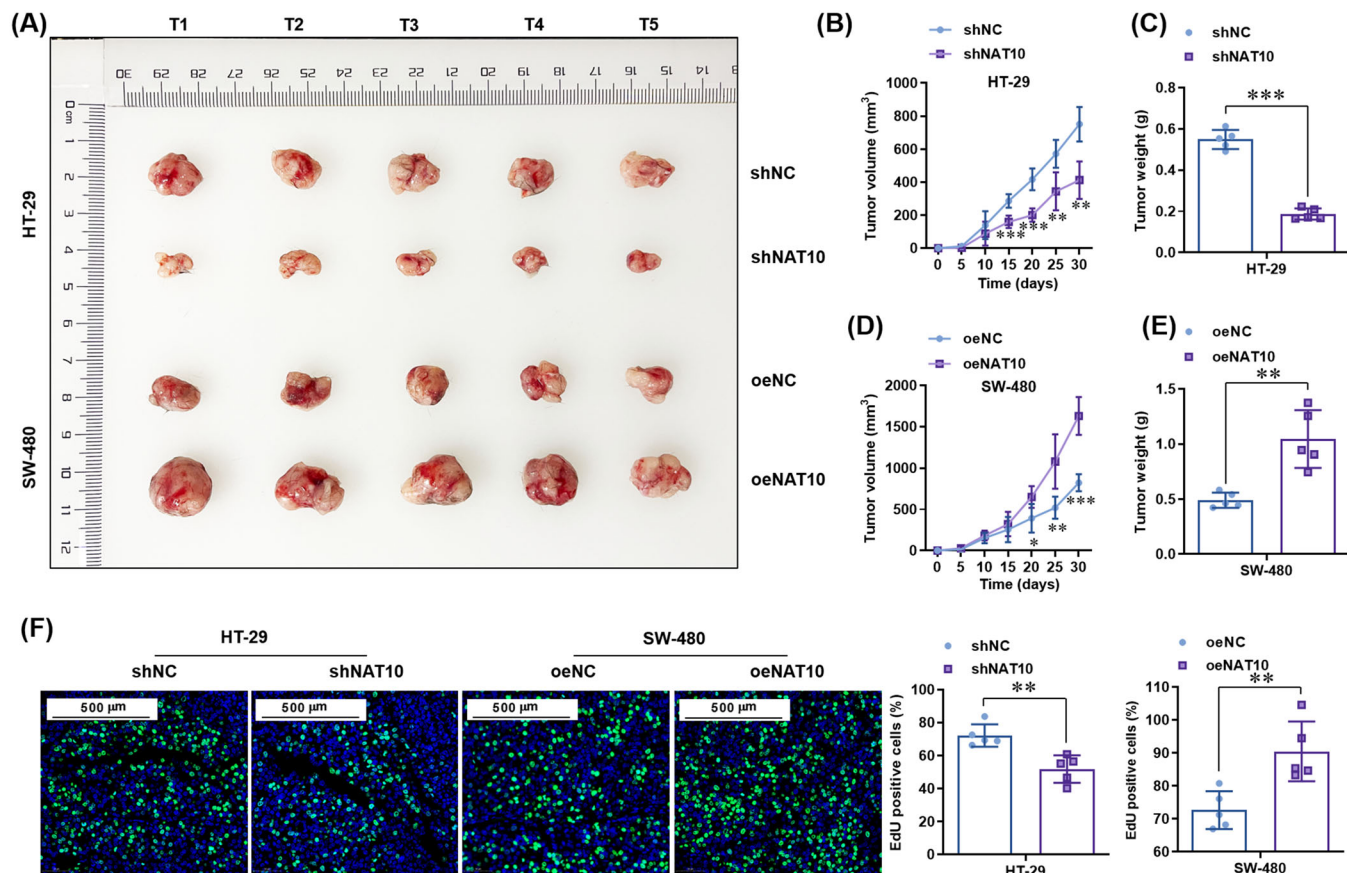
FIGURE 3 *NAT10* promotes the tumorigenesis of colon cancer cells in vivo. (A) Subcutaneous transplantation tumor models in nude mice were used to evaluate the effects of *NAT10* knockdown and overexpression on the tumorigenesis of colon cancer cells. The tumors derived from HT-29 (shNC and sh*NAT10*) and SW-480 (oeNC and oe*NAT10*) cells were isolated ($n = 5$ in each group). (B, D) The growth of tumors derived from HT-29 and SW-480 cells was plotted every five days after subcutaneous injection. (C, E) The weights of tumors derived from HT-29 and SW-480 cells were analyzed. (F) The numbers of EdU-positive cells were quantified in tumors derived from HT-29 (shNC and sh*NAT10*) and SW-480 (oeNC and oe*NAT10*) cells. *$P < 0.05$, **$P < 0.01$, and ***$P < 0.001$. Abbreviations: *NAT10*, N-acetyltransferase 10; shNC, knockdown negative control, sh*NAT10*, *NAT10* knockdown; oeNC, overexpression control; oe*NAT10*, *NAT10* overexpression; EdU, 5-ethynyl-2′-deoxyuridine.

showed that *NAT10* knockdown failed to decrease the luciferase activity of the construct with the C132A mutation in the ac4C site (Figure 5J). Collectively, these results suggest that *NAT10* improves the stability of *FSP1* mRNA and enhances its expression in colon cancer cells.

3.5 │ *NAT10* knockdown significantly increased ferroptosis in colon cancer cells

Considering that *FSP1* is a glutathione-independent ferroptosis suppressor [41, 42], we explored whether *NAT10* alters the level of ferroptosis. We measured the levels of intracellular ROS, GSH, and malondialdehyde (MDA), an oxidative stress marker, in *NAT10*-knockdown HT-29 and LoVo cells. The intensity of DCFH-DA indicated that lipid ROS levels were significantly increased in *NAT10*-knockdown HT-29 and LoVo cells compared to vector con-

trol HT-29 and LoVo cells (Figure 6A). In addition, ferrous iron (Figure 6B), GSH depletion (Figure 6C), and MDA levels (Figure 6D) were significantly increased after *NAT10* knockdown. Furthermore, TEM was performed, and the results showed mitochondrial matrix condensation and the formation of enlarged cristae in *NAT10*-knockdown HT-29 and LoVo cells (Figure 6E). Taken together, these findings strongly suggest that *NAT10* knockdown triggers ferroptosis in colon cancer cells.

3.6 │ Ferroptosis inhibition reversed the suppressive effects of *NAT10* knockdown on the proliferation and metastasis of colon cancer cells both in vitro and in vivo

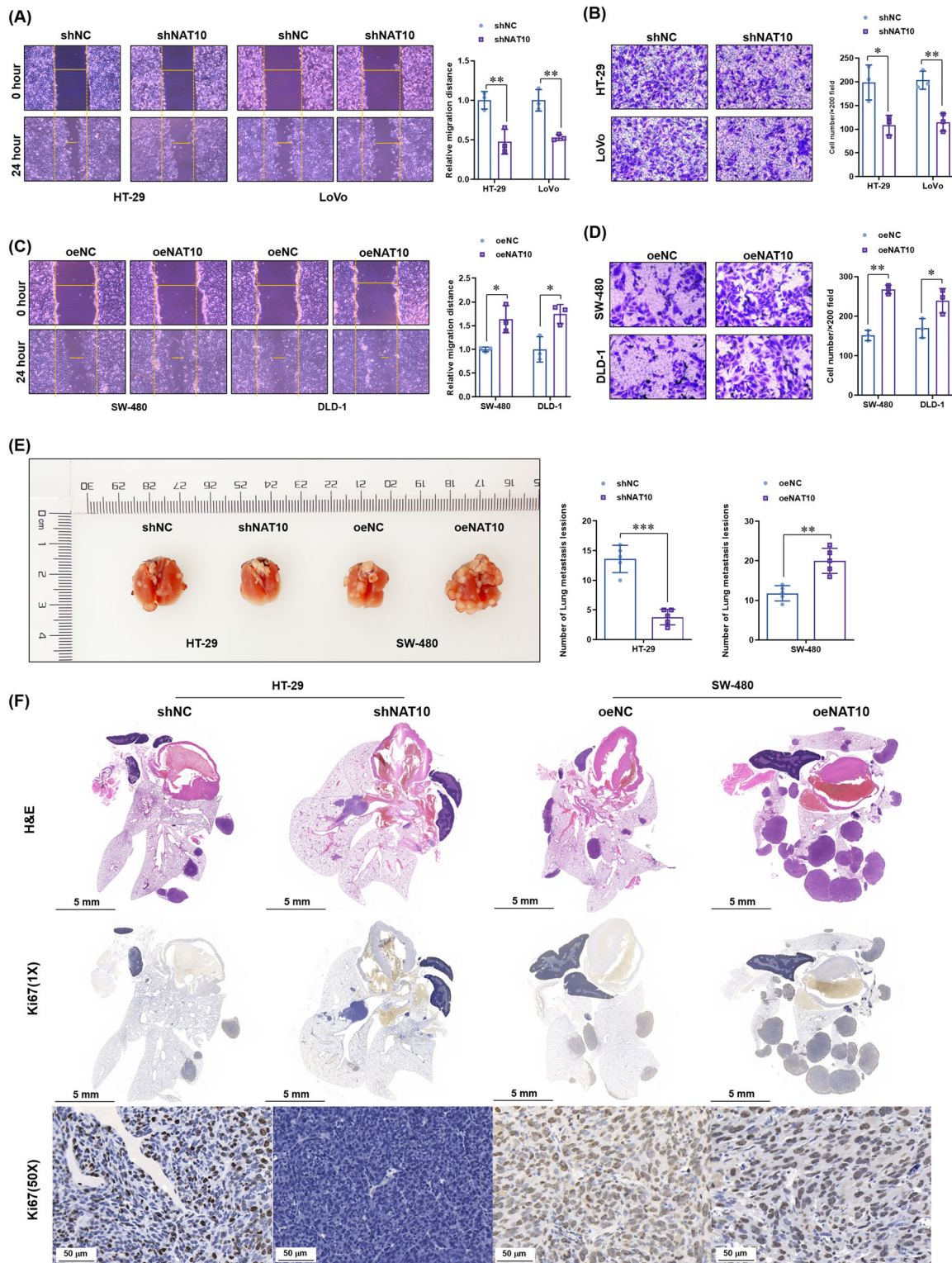To further confirm whether ferroptosis contributes to the suppression of colon cancer cell proliferation after

FIGURE 4 *NAT10* promotes the metastasis of colon cancer cells both in vitro and in vivo. (A) The effect of *NAT10* knockdown on the migration of HT-29 and LoVo cells was evaluated using a wound healing assay ($n = 3$). (B) The role of *NAT10* knockdown on the invasion of HT-29 and LoVo cells was analyzed by Transwell invasion assay ($n = 3$). (C) The effect of *NAT10* overexpression on the migration of SW480 and DLD-1 cells was evaluated using a wound healing assay ($n = 3$). (D) The role of *NAT10* overexpression on the invasion of SW480 and DLD-1 cells was analyzed by Transwell invasion assay ($n = 3$). (E) HT29 (shNC and sh*NAT10*) and SW480 (oeNC and oe*NAT10*) cells were injected into the tail vein of nude mice to determine the metastatic ability of colon cancer cells. The lungs with metastatic lesions were isolated ($n = 5$). (F) Histopathological diagnosis was performed using H&E staining and Ki67 staining to show proliferation in the lung metastatic lesions ($n = 5$). *$P < 0.05$, **$P < 0.01$ and ***$P < 0.001$. Abbreviations: *NAT10*, N-acetyltransferase 10; H&E, hematoxylin and eosin staining; shNC, knockdown negative control, sh*NAT10*, *NAT10* knockdown; oeNC, overexpression control; oe*NAT10*, *NAT10* overexpression.
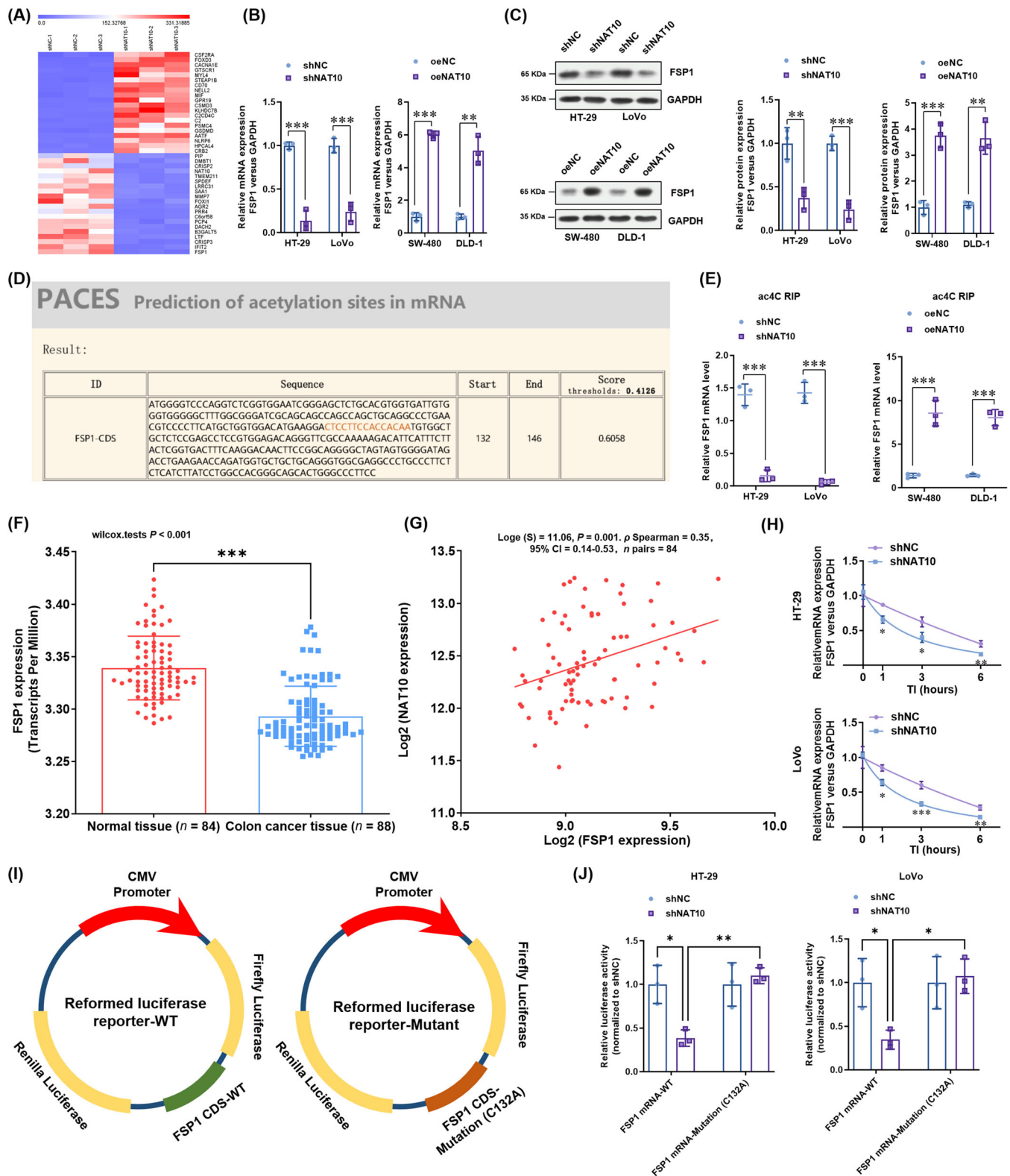
FIGURE 5 *NAT10* improves *FSP1* mRNA stability and enhances its expression in colon cancer cells. (A) A transcriptomic comparison was carried out to analyze the dysregulated genes between *NAT10*-knockdown and vector control HT-29 cells, and the results are shown using a volcano map. (B) The *FSP1* mRNA levels in *NAT10*-knockdown HT-29 and LoVo cells and *NAT10*-overexpressing SW480 and DLD-1 cells were verified by real-time PCR (*n* = 3). (C) The *FSP1* protein levels in *NAT10*-knockdown HT-29 and LoVo cells and *NAT10*-overexpressing SW480 and DLD-1 cells were verified by Western blotting analysis (*n* = 3). (D) PACES tools (http://rnanut.net/paces/) were used to predict the conserved acetylation sites in the *FSP1* mRNA CDS. (E) ac4C RIP-PCR was used to analyze the level of ac4C in acetylated *FSP1* mRNA in *NAT10*-knockdown HT-29 and LoVo cells and *NAT10*-overexpressing SW-480 and DLD-1 cells (*n* = 3). (F-G) The expression of *FSP1* and its

NAT10 knockdown, we treated colon cancer cells with a specific ferroptosis inhibitor (ferrostatin-1, 2 μmol/L). As expected, inhibition of ferroptosis by ferrostatin-1 did not affect cell proliferation, as indicated by the CCK-8 assay (Figure 7A) and colony formation assay (Figure 7B). However, cell proliferation was significantly increased by ferrostatin-1 in *NAT10*-knockdown HT-29 and LoVo cells (Figure 7A-B). Interestingly, in the subcutaneous transplantation tumor model in nude mice, ferrostatin-1 significantly improved the growth (Figure 7C-D) and increased the weight (Figure 7E) of the tumors derived from the vector control HT-29 cells. Moreover, ferrostatin-1 significantly abrogated the inhibitory effect of *NAT10* knockdown on the growth (Figure 7D) and weight (Figure 7E) of tumors derived from *NAT10*-knockdown HT-29 cells. Consistently, the EdU incorporation assay showed that *NAT10* knockdown reduced the proliferation of cells in the tumors derived from HT-29 cells, and this effect was reversed by ferrostatin-1 treatment (Figure 7F). Regarding ferroptosis, *NAT10* knockdown-increased serum levels of LDH (Figure 7G) and ferrous iron (Figure 7H) were significantly reversed by ferrostatin-1, whereas it did not affect the CRP level (Figure 7I). These results demonstrate that inhibition of ferroptosis reversed the *NAT10* knockdown-mediated suppression of proliferation in colon cancer cells both in vitro and in vivo.

Furthermore, we determined whether ferroptosis contributes to the suppression of metastasis by *NAT10* knockdown in colon cancer cells in vitro and in vivo. The results showed that ferrostatin-1 did not affect the migration and invasion of the vector control HT-29 and LoVo cells, but it significantly increased the migration distance and invasion of *NAT10*-knockdown HT-29 and LoVo cells (Figure 8A-B). Similar to the in vitro results, ferrostatin-1 did not affect the number of lung metastasis lesions derived from the vector control HT-29 cells, but increased the lesions derived from *NAT10*-knockdown HT-29 cells (Figure 8C). Histopathological diagnosis further confirmed the effect of ferrostatin-1 in promoting the growth of *NAT10*-knockdown HT-29 cells (Figure 8D). Simultaneously, Ki67 staining showed proliferation in the resected lung tissues, which was not altered by ferrostatin-1 treatment, in the vector control HT-29 group. Ferrostatin-

1 enhanced the proliferation in lung metastasis lesions derived from *NAT10*-knockdown HT-29 cells (Figure 8D). Collectively, these results suggest that the inhibition of ferroptosis reversed the *NAT10* knockdown-mediated suppression of proliferation and metastasis of colon cancer cells both in vitro and in vivo (Figure 8E).

4 | DISCUSSION

In this study, we revealed several interesting findings regarding the oncogenic functions of *NAT10* in the growth and metastasis of colon cancer. We found that *NAT10* was upregulated in cancer tissues and cell lines, and upregulated *NAT10* expression was associated with shorter survival of colon cancer patients. Functionally, an oncogenic role of *NAT10* was revealed in in vitro and in vivo experiments that investigated the proliferation and metastasis of colon cancer cells. Regarding molecular mechanisms, the *FSP1* mRNA stability and expression in colon cancer cells were found to be improved by *NAT10*-mediated ac4C acetylation. Moreover, the results showed that inhibition of ferroptosis by *FSP1* is critical to the *NAT10*-mediated improvement of proliferation and metastasis of colon cancer cells.

Colon cancer has a high mortality, and its incidence is increasing worldwide [2, 3]. Despite advances in colon cancer treatment over the past few decades, the mortality of colon cancer is still very high, mainly due to recurrence and distant organ metastases [6, 8]. *NAT10* is a histone acetyltransferase which is mainly localized to the nucleoli and is involved in many biological processes [13, 15]. Evidence suggests that *NAT10* can bind to acetyltransferases and RNA, and it is the only enzyme that can catalyze the ac4C modification of eukaryotic RNA [12]. Studies have also shown that ac4C acetylation, an mRNA modification, regulated telomerase activity, RNA synthesis, DNA damage repair, and mRNA stability [12, 43]. It is also associated with the development, progression, and prognosis of various human diseases, especially cancer [19, 44, 45]. Given that it is the only acetyltransferase that catalyzes the ac4C modification, *NAT10* is significantly associated with the prognosis of a variety of malignant

---

correlation with *NAT10* expression in colon cancer tumor tissues from the GEO dataset (GSE31782) were analyzed. (H) The percentages of remaining mRNA versus the mRNA levels after the addition of actinomycin D (0, 1, 3 and 6 h) were quantified to analyze *FSP1* mRNA stability ($n = 3$). (I) Schematic illustration of the establishment of the two reformed luciferase reporter plasmids by inserting partial *FSP1* mRNA sequences with wild-type or C132A mutated ac4C sites. (J) The luciferase activity was measured ($n = 3$). *$P < 0.05$, **$P < 0.01$, and ***$P < 0.001$. Abbreviations: shNC, knockdown negative control, sh*NAT10*, *NAT10* knockdown; oeNC, overexpression control; oe*NAT10*, *NAT10* overexpression; KDa, kilodalton; RIP, RNA immunoprecipitation; *NAT10*, N-acetyltransferase 10; *FSP1*, ferroptosis suppressor protein 1; ac4C RIP, N4-acetylcytidine RNA immunoprecipitation; TI: transcription inhibition assay; mRNA, messenger RNA; WT, wildtype; CDS, coding sequence.
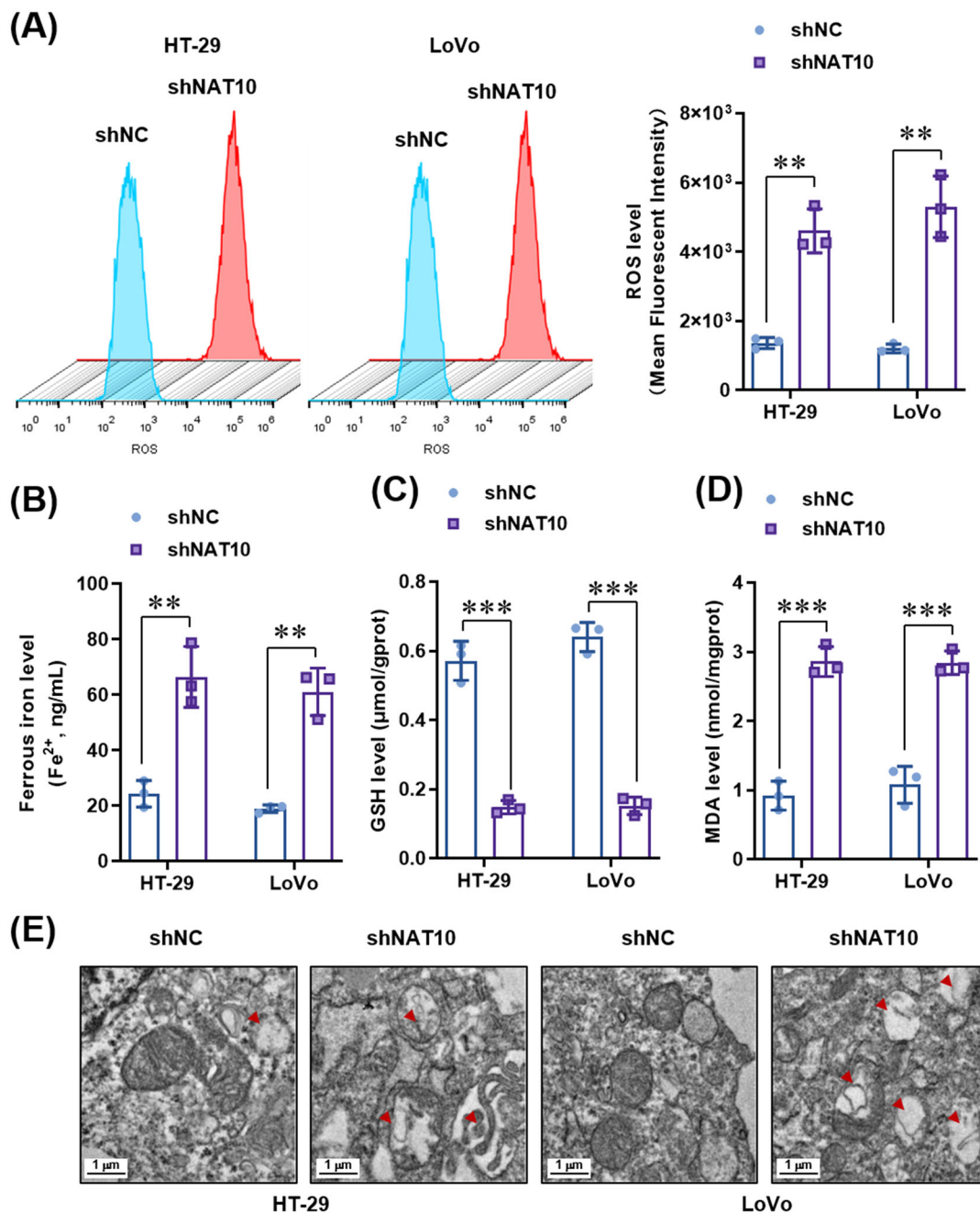
FIGURE 6 *NAT10* knockdown significantly activates ferroptosis in colon cancer cells. (A-D) The levels of intracellular ROS (A), ferrous iron (B), GSH (C), and MDA (D) in *NAT10*-knockdown HT-29 and LoVo cells ($n = 3$). (E) Representative TEM images showing mitochondrial matrix condensation and the formation of enlarged cristae (red arrowheads) in *NAT10*-knockdown HT-29 and LoVo cells ($n = 3$). **$P < 0.01$ and ***$P < 0.001$. Abbreviations: shNC, knockdown negative control, sh*NAT10*, *NAT10* knockdown; *NAT10*, N-acetyltransferase 10; Fe^{2+}, ferrous iron; ROS, reactive oxygen species; GSH, glutathione; MDA, malondialdehyde; TEM, transmission electron microscopy.

tumors and may promote tumor progression. High expression of *NAT10* in liver cancer [19], breast cancer [16], gastric cancer [26], and head and neck squamous cell carcinoma [46] was associated with poor prognosis. However, few studies have explored the role of *NAT10* in colon cancer. Zhang *et al.* [29] reported that glycogen synthase kinase-3beta-regulated *NAT10* was involved in colorectal cancer invasion. Cao *et al.* [47] found that *NAT10* promoted

micronucleus formation, activated mechanism underlying the senescence-related secretion phenotype, and promoted colorectal cancer progression. Similar to our observations, these authors found that downregulation of *NAT10* inhibited cell proliferation according to cell cycle and BrdU incorporation assays. Furthermore, they showed a critical role of *NAT10* under the conditions of oxidative stress or DNA damage. The present study demonstrated that *NAT10*
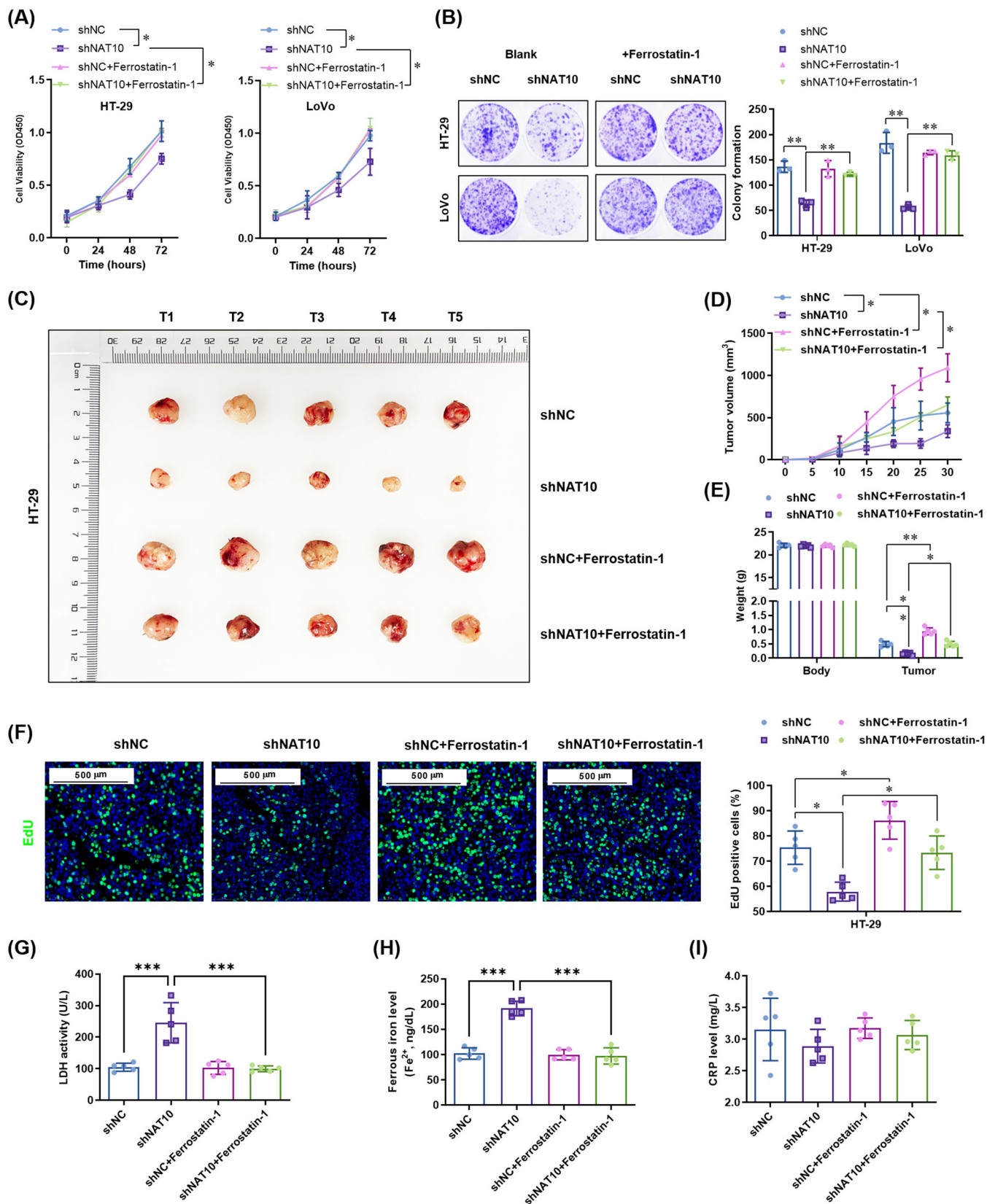
FIGURE 7 Inhibition of ferroptosis reverses the *NAT10* knockdown-mediated suppression of proliferation in colon cancer cells both in vitro and in vivo. (A) A CCK-8 assay was used to analyze the effect of ferrostatin-1 on the proliferation of *NAT10*-knockdown colon cancer cells ($n = 3$). (B) A colony formation assay was used to verify the effect of ferrostatin-1 on the proliferation of *NAT10*-knockdown colon cancer cells ($n = 3$). (C) A subcutaneous transplantation tumor model was used to evaluate the effect of ferrostatin-1 on the tumorigenesis of

was upregulated in colon cancer tissues and cell lines, and high expression of *NAT10* was associated with short survival according to a tissue microarray analysis. The expression of *NAT10* was also related to lymph node metastasis, clinical stage, and T stage. Interestingly, it seems that the difference appeared later during patient follow-up, which may suggest a limited prognostic value of *NAT10* in colon cancer. Furthermore, it was found that knockdown of *NAT10* in the colon cancer cell lines with low expression levels (HT-29 and LoVo) impaired the proliferation, migration, and invasion of the cells, whereas overexpression of *NAT10* in the colon cancer cell lines with high expression (SW480 and DLD-1) promoted these activities both in in vitro experiments and xenograft models. Collectively, these results suggest an oncogenic role of *NAT10* in colon cancer.

To further explore the mechanism by which *NAT10* contributes to the progression of colon cancer, we performed a transcriptomic comparison between *NAT10*-knockdown and vector control HT-29 cells. The results showed a significant decrease in the expression of *FSP1*, also known as apoptosis-inducing factor mitochondria-associated 2 (AIFM2), in *NAT10*-knockdown HT-29 cells. Notably, a recent study revealed *FSP1* as a glutathione-independent ferroptosis suppressor [42]. Ferroptosis is an iron-dependent form of necrotic cell death characterized by phospholipid oxidative damage, and it is antagonized by glutathione peroxidase 4 (*GPX4*) and *FSP1*. In addition, tumor cells that survive other forms of cell death are known to become or remain resistant to ferroptosis [48]. In recent years, there has been evidence that ferroptosis was associated with a multitude of cancers, including head and neck squamous cell carcinoma [30], renal cell carcinoma [39], breast cancer [49], lung cancer [50], pancreatic cancer [51], and diffuse large B-cell lymphoma [52]. Additionally, researchers have found that CD8+ T cell activation increased ferroptosis-specific lipid peroxidation in tumor cells, activating ferroptosis and contributing to the effectiveness of immunotherapy against tumors [53]. Therefore, the therapeutic exploitation of ferroptosis in cancer has become a research hotspot. The present study has shown that *NAT10* knockdown significantly induced ferroptosis in colon cancer cells. Moreover, inhibition of ferroptosis using ferrostatin-1 reversed the *NAT10* knockdown-mediated suppression of proliferation

and metastasis in colon cancer cells both in vitro and in vivo. Interestingly, ferrostatin-1 did not affect the proliferation of colon cancer cells in vitro, but it promoted the tumorigenesis of colon cancers in a subcutaneous transplantation tumor model in nude mice. This result suggests a more complicated role of ferroptosis in the progression of colon cancer in vivo.

Dysregulation of programmed cell death may largely affect the efficiency of colon cancer treatment [48]. Emerging studies have shown that activation of ferroptosis-related pathways was effective in preventing tumor progression and enhancing the benefits of chemotherapy, targeted therapy, and even immunotherapy in colon cancer patients [53]. It is certainly interesting to determine whether *NAT10*-regulated ferroptosis can improve the therapeutic effect of chemotherapy, targeted therapy, and immunotherapy in colon cancer, and this topic needs further study.

Meanwhile, we recognize some limitations of the present study. Firstly, the in vivo study was performed with a cell line-derived xenograft in Balb/c NOD mice. Colon cancer patient-derived xenograft (PDX) models would be more helpful to understand the critical role of *NAT10* in colon cancer progression. Secondly, we concluded that *FSP1* is the major target of *NAT10*-mediated acetylation in the regulation of ferroptosis in colon cancer cells, further evaluation of some other functional acetylated RNAs is required. Thirdly, following dramatic success in many types of advanced solid tumors, immunotherapy has rapidly become established as a major treatment modality for multiple types of solid cancers. Ferroptosis is a promising target for cancer immunotherapy. It would be interesting to identify whether *NAT10*-*FSP1*-ferroptosis signaling regulates the immunotherapy efficiency in colon cancer.

5 | CONCLUSIONS

Our present study revealed that *NAT10* was upregulated in colon cancer tissues and associated with shorter patient survival. We found that *NAT10* promoted the proliferation and metastasis abilities of colon cells by increasing the mRNA stability and expression of *FSP1*, indicating

NAT10-knockdown colon cancer cells. Tumors derived from normal HT-29 (shNC and sh*NAT10*) and ferrostatin-1-treated HT-29 (shNC and sh*NAT10*) cells were isolated ($n = 5$). (D) The volume of tumors derived from HT-29 cells was plotted every five days after subcutaneous injection ($n = 5$). (E) The body weights of the mice and the weights of tumors derived from HT-29 cells were analyzed ($n = 5$). (F) EdU-positive cell numbers were quantified in the tumors derived from HT-29 (shNC and sh*NAT10*) cells with and without ferrostatin-1 treatment ($n = 5$). (G-I) The serum levels of LDH (G), ferrous iron (H) and CRP (I) were analyzed. *$P < 0.05$, **$P < 0.01$ and ***$P < 0.001$. Abbreviations: shNC, knockdown negative control, sh*NAT10*, *NAT10* knockdown; oeNC, overexpression control; oe*NAT10*, *NAT10* overexpression; *NAT10*, N-acetyltransferase 10; EdU, 5-ethynyl-2′-deoxyuridine; LDH, Lactate dehydrogenase; CRP, C-reaction protein; Fe^{2+}, ferrous iron.
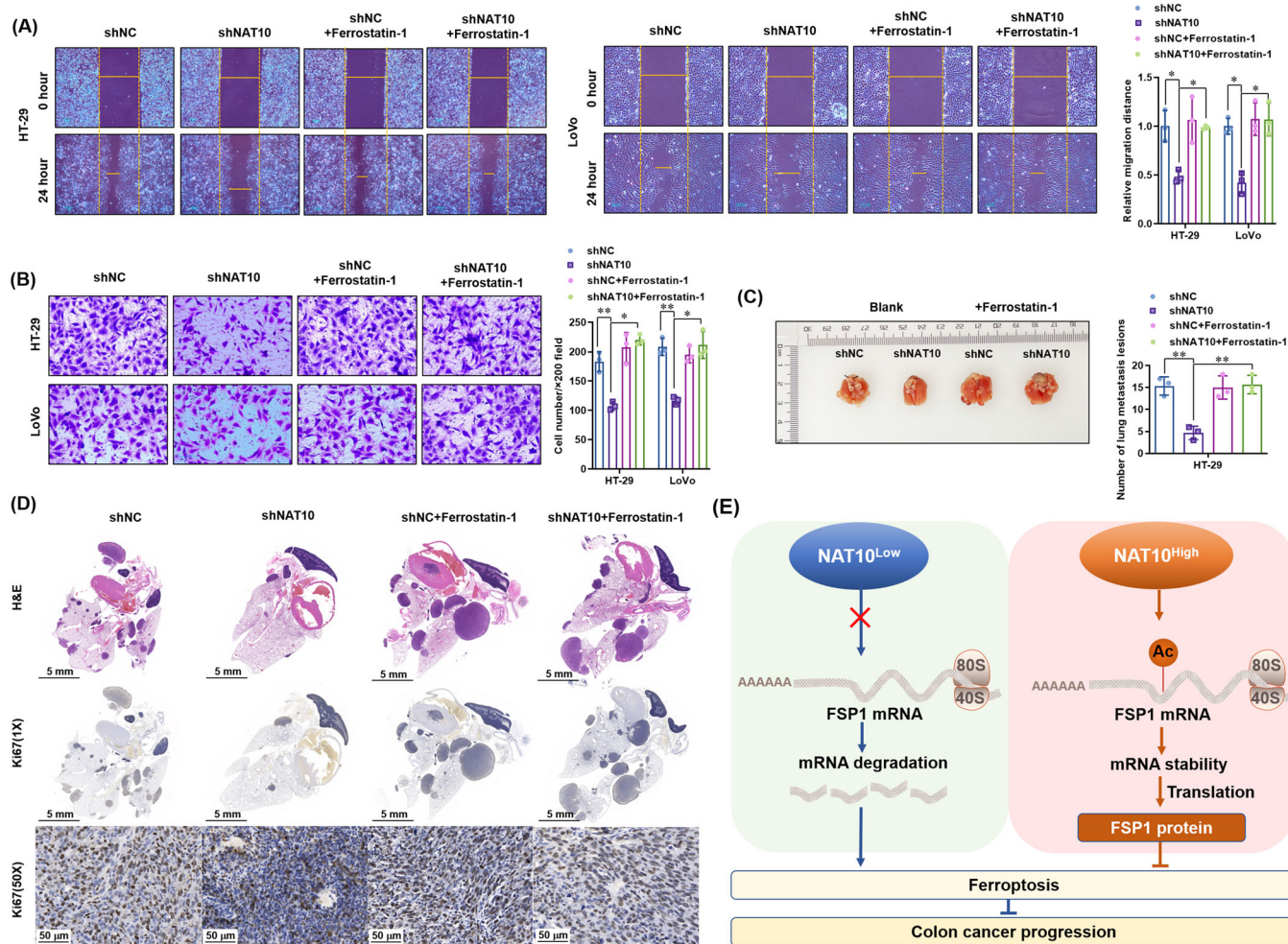
FIGURE 8 Inhibition of ferroptosis reverses the *NAT10* knockdown-mediated suppression of proliferation and metastasis in colon cancer cells both in vitro and in vivo. (A) The effect of ferrostatin-1 on the migration of *NAT10*-knockdown colon cancer cells was evaluated using a wound healing assay ($n = 3$). (B) The role of ferrostatin-1 in the invasion of *NAT10*-knockdown colon cancer cells was analyzed by Transwell invasion assay ($n = 3$). (C) HT-29 (shNC and sh*NAT10*) cells were injected into the tail vein of nude mice, and ferrostatin-1 (1 mg/kg) was injected every five days to explore the effect of ferrostatin-1 on the metastatic ability of HT-29 (shNC and sh*NAT10*) cells. Next, the lungs with metastatic lesions were isolated ($n = 5$). (D) Histopathological diagnosis was performed using H&E staining (1×) and Ki67 staining (1× and 20×) to show proliferation in the lung metastatic lesions ($n = 5$). (E) A graphical abstract showing the mechanism by which *NAT10*-mediated N4 acetylation of *FSP1* mRNA inhibits ferroptosis of colon cancer cells. *$P < 0.05$ and **$P < 0.01$. Abbreviations: shNC, knockdown negative control, sh*NAT10*, *NAT10* knockdown; NAT10, N-acetyltransferase 10; *FSP1*, ferroptosis suppressor protein 1; H&E, hematoxylin and eosin staining; Ac, acetylation.

that *NAT10-FSP1*-ferroptosis signaling is a novel mechanism underlying tumor growth and metastasis in colon cancer.

DECLARATIONS

AUTHOR CONTRIBUTIONS
Jingting Jiang and Xiao Zheng designed this study. Xiao Zheng performed all the experiments; Xiao Zheng, Qi Wang, You Zhou, and Dachuan Zhang collected the tissue samples and the clinical data; Yiting Geng and Wenwei Hu analyzed and interpreted the data; Xiao Zheng and Jingting Jiang drafted the manuscript; Changping Wu and Yufang Shi analyzed the data and revised the manuscript. All the authors read and approved the final manuscript.

(QN202103), and the open fund of state key laboratory of Pharmaceutical Biotechnology, Nanjing University, China (KF-202203).

COMPETING INTERESTS
The authors declare no conflicts of interest.

AVAILABILITY OF DATA AND MATERIALS
The corresponding author will provide all the data used in this study upon request.

ETHICS APPROVAL AND CONSENT TO PARTICIPATE
Each patient who participated in the study provided written informed consent for the biological studies, and the study was approved by the Ethics Committee at the Third Affiliated Hospital of Soochow University (2019-003). The animal experiments conducted at the Third Affiliated Hospital of Soochow University were approved by the Animal Experimental Committee of the Third Affiliated Hospital of Soochow University (2019-003).

CONSENT FOR PUBLICATION
Not applicable.

ORCID
Jingting Jiang https://orcid.org/0000-0002-3128-9762

REFERENCES
1. Bien J, Lin A. A Review of the Diagnosis and Treatment of Metastatic Colorectal Cancer. JAMA. 2021;325(23):2404-5.
2. Chen W, Zheng R, Baade PD, Zhang S, Zeng H, Bray F, et al. Cancer statistics in China, 2015. CA Cancer J Clin. 2016;66(2):115-32.
3. Siegel RL, Miller KD, Jemal A. Cancer statistics, 2020. CA Cancer J Clin. 2020;70(1):7-30.
4. Qiu H, Cao S, Xu R. Cancer incidence, mortality, and burden in China: a time-trend analysis and comparison with the United States and United Kingdom based on the global epidemiological data released in 2020. Cancer Commun (Lond). 2021;41(10):1037-48.
5. Angenete E. Who should manage post-treatment care for patients with colon cancer: surgeons or general practitioners? Lancet Oncol. 2021;22(8):1053-4.
6. Cardoso R, Guo F, Heisser T, Hackl M, Ihle P, De Schutter H, et al. Colorectal cancer incidence, mortality, and stage distribution in European countries in the colorectal cancer screening era: an international population-based study. Lancet Oncol. 2021;22(7):1002-13.
7. Goc J, Lv M, Bessman NJ, Flamar AL, Sahota S, Suzuki H, et al. Dysregulation of ILC3s unleashes progression and immunotherapy resistance in colon cancer. Cell. 2021;184(19):5015-30 e16.
8. Kerr DJ, Chamberlain S, Kerr RS. Celecoxib for Stage III Colon Cancer. JAMA. 2021;325(13):1257-8.
9. Osman A, Yan B, Li Y, Pavelko KD, Quandt J, Saadalla A, et al. TCF-1 controls Treg cell functions that regulate inflammation, CD8(+) T cell cytotoxicity and severity of colon cancer. Nat Immunol. 2021;22(9):1152-62.
10. Schmitt M, Greten FR. The inflammatory pathogenesis of colorectal cancer. Nat Rev Immunol. 2021;21(10):653-67.
11. Sinicrope FA, Graham RP. Tumor-Infiltrating Lymphocytes for Prognostic Stratification in Nonmetastatic Colon Cancer-Are We There Yet? JAMA Oncol. 2021;7(7):969-70.
12. Arango D, Sturgill D, Alhusaini N, Dillman AA, Sweet TJ, Hanson G, et al. Acetylation of Cytidine in mRNA Promotes Translation Efficiency. Cell. 2018;175(7):1872-86 e24.
13. Balmus G, Larrieu D, Barros AC, Collins C, Abrudan M, Demir M, et al. Targeting of NAT10 enhances healthspan in a mouse model of human accelerated aging syndrome. Nat Commun. 2018;9(1):1700.
14. Dalhat MH, Mohammed MRS, Ahmad A, Khan MI, Choudhry H. Remodelin, a N-acetyltransferase 10 (NAT10) inhibitor, alters mitochondrial lipid metabolism in cancer cells. J Cell Biochem. 2021.
15. Larrieu D, Britton S, Demir M, Rodriguez R, Jackson SP. Chemical inhibition of NAT10 corrects defects of laminopathic cells. Science. 2014;344(6183):527-32.
16. Liu HY, Liu YY, Yang F, Zhang L, Zhang FL, Hu X, et al. Acetylation of MORC2 by NAT10 regulates cell-cycle checkpoint control and resistance to DNA-damaging chemotherapy and radiotherapy in breast cancer. Nucleic Acids Res. 2020;48(7):3638-56.
17. Liu X, Cai S, Zhang C, Liu Z, Luo J, Xing B, et al. Deacetylation of NAT10 by Sirt1 promotes the transition from rRNA biogenesis to autophagy upon energy stress. Nucleic Acids Res. 2018;46(18):9601-16.
18. Liu X, Tan Y, Zhang C, Zhang Y, Zhang L, Ren P, et al. NAT10 regulates p53 activation through acetylating p53 at K120 and ubiquitinating Mdm2. EMBO Rep. 2016;17(3):349-66.
19. Zhang X, Chen J, Jiang S, He S, Bai Y, Zhu L, et al. N-Acetyltransferase 10 Enhances Doxorubicin Resistance in Human Hepatocellular Carcinoma Cell Lines by Promoting the Epithelial-to-Mesenchymal Transition. Oxid Med Cell Longev. 2019;2019:7561879.
20. Yang W, Li HY, Wu YF, Mi RJ, Liu WZ, Shen X, et al. ac4C acetylation of RUNX2 catalyzed by NAT10 spurs osteogenesis of BMSCs and prevents ovariectomy-induced bone loss. Mol Ther Nucleic Acids. 2021;26:135-47.
21. Sas-Chen A, Thomas JM, Matzov D, Taoka M, Nance KD, Nir R, et al. Dynamic RNA acetylation revealed by quantitative cross-evolutionary mapping. Nature. 2020;583(7817):638-43.
22. Thomas JM, Briney CA, Nance KD, Lopez JE, Thorpe AL, Fox SD, et al. A Chemical Signature for Cytidine Acetylation in RNA. J Am Chem Soc. 2018;140(40):12667-70.
23. Tsai K, Jaguva Vasudevan AA, Martinez Campos C, Emery A, Swanstrom R, Cullen BR. Acetylation of Cytidine Residues Boosts HIV-1 Gene Expression by Increasing Viral RNA Stability. Cell Host Microbe. 2020;28(2):306-12 e6.
24. Montgomery DC, Garlick JM, Kulkarni RA, Kennedy S, Allali-Hassani A, Kuo YM, et al. Global Profiling of Acetyltransferase Feedback Regulation. J Am Chem Soc. 2016;138(20):6388-91.
25. Sharma S, Langhendries JL, Watzinger P, Kotter P, Entian KD, Lafontaine DL. Yeast Kre33 and human NAT10 are conserved 18S rRNA cytosine acetyltransferases that modify tRNAs

assisted by the adaptor Tan1/THUMPD1. Nucleic Acids Res. 2015;43(4):2242-58.

26. Zhang Y, Jing Y, Wang Y, Tang J, Zhu X, Jin WL, et al. NAT10 promotes gastric cancer metastasis via N4-acetylated COL5A1. Signal Transduct Target Ther. 2021;6(1):173.

27. Larrieu D, Vire E, Robson S, Breusegem SY, Kouzarides T, Jackson SP. Inhibition of the acetyltransferase NAT10 normalizes progeric and aging cells by rebalancing the Transportin-1 nuclear import pathway. Sci Signal. 2018;11(537).

28. Xiang Y, Zhou C, Zeng Y, Guo Q, Huang J, Wu T, et al. NAT10-Mediated N4-Acetylcytidine of RNA Contributes to Post-transcriptional Regulation of Mouse Oocyte Maturation in vitro. Front Cell Dev Biol. 2021;9:704341.

29. Zhang H, Hou W, Wang HL, Liu HJ, Jia XY, Zheng XZ, et al. GSK-3beta-regulated N-acetyltransferase 10 is involved in colorectal cancer invasion. Clin Cancer Res. 2014;20(17):4717-29.

30. Chen X, Kang R, Kroemer G, Tang D. Broadening horizons: the role of ferroptosis in cancer. Nat Rev Clin Oncol. 2021;18(5):280-96.

31. Garcia-Bermudez J, Birsoy K. A mitochondrial gatekeeper that helps cells escape death by ferroptosis. Nature. 2021;593(7860):514-5.

32. Jiang X, Stockwell BR, Conrad M. Ferroptosis: mechanisms, biology and role in disease. Nat Rev Mol Cell Biol. 2021;22(4):266-82.

33. Mao C, Lei G, Zhuang L, Gan B. Phospholipase iPLA2beta acts as a guardian against ferroptosis. Cancer Commun (Lond). 2021;41(11):1082-5.

34. Tang D, Chen X, Kang R, Kroemer G. Ferroptosis: molecular mechanisms and health implications. Cell Res. 2021;31(2):107-25.

35. Aldrovandi M, Conrad M. Ferroptosis: the Good, the Bad and the Ugly. Cell Res. 2020;30(12):1061-2.

36. Zheng J, Conrad M. The Metabolic Underpinnings of Ferroptosis. Cell Metab. 2020;32(6):920-37.

37. Koren E, Fuchs Y. Modes of Regulated Cell Death in Cancer. Cancer Discov. 2021;11(2):245-65.

38. Lange M, Olzmann JA. Ending on a sour note: Lipids orchestrate ferroptosis in cancer. Cell Metab. 2021;33(8):1507-9.

39. Reznik E, Jiang H, Hakimi AA. Chemerin Tips the Scales in ccRCC to Evade Ferroptosis. Cancer Discov. 2021;11(8):1879-80.

40. Zheng X, Chen L, Zhou Y, Wang Q, Zheng Z, Xu B, et al. A novel protein encoded by a circular RNA circPPP1R12A promotes tumor pathogenesis and metastasis of colon cancer via Hippo-YAP signaling. Mol Cancer. 2019;18(1):47.

41. Bersuker K, Hendricks JM, Li Z, Magtanong L, Ford B, Tang PH, et al. The CoQ oxidoreductase FSP1 acts parallel to GPX4 to inhibit ferroptosis. Nature. 2019;575(7784):688-92.

42. Doll S, Freitas FP, Shah R, Aldrovandi M, da Silva MC, Ingold I, et al. FSP1 is a glutathione-independent ferroptosis suppressor. Nature. 2019;575(7784):693-8.

43. Wiener D, Schwartz S. The epitranscriptome beyond m(6)A. Nat Rev Genet. 2021;22(2):119-31.

44. Bortolin-Cavaille ML, Quillien A, Thalalla Gamage S, Thomas JM, Sas-Chen A, Sharma S, et al. Probing small ribosomal subunit RNA helix 45 acetylation across eukaryotic evolution. Nucleic Acids Res. 2022;50(11):6284-99.

45. Wang G, Zhang M, Zhang Y, Xie Y, Zou J, Zhong J, et al. NAT10-mediated mRNA N4-acetylcytidine modification promotes bladder cancer progression. Clin Transl Med. 2022;12(5):e738.

46. Tao W, Tian G, Xu S, Li J, Zhang Z, Li J. NAT10 as a potential prognostic biomarker and therapeutic target for HNSCC. Cancer Cell Int. 2021;21(1):413.

47. Cao Y, Yao M, Wu Y, Ma N, Liu H, Zhang B. N-Acetyltransferase 10 Promotes Micronuclei Formation to Activate the Senescence-Associated Secretory Phenotype Machinery in Colorectal Cancer Cells. Transl Oncol. 2020;13(8):100783.

48. Liang C, Zhang X, Yang M, Dong X. Recent Progress in Ferroptosis Inducers for Cancer Therapy. Adv Mater. 2019;31(51):e1904197.

49. Li Z, Chen L, Chen C, Zhou Y, Hu D, Yang J, et al. Targeting ferroptosis in breast cancer. Biomark Res. 2020;8(1):58.

50. Chen P, Wu Q, Feng J, Yan L, Sun Y, Liu S, et al. Erianin, a novel dibenzyl compound in Dendrobium extract, inhibits lung cancer cell growth and migration via calcium/calmodulin-dependent ferroptosis. Signal Transduct Target Ther. 2020;5(1):51.

51. Badgley MA, Kremer DM, Maurer HC, DelGiorno KE, Lee HJ, Purohit V, et al. Cysteine depletion induces pancreatic tumor ferroptosis in mice. Science. 2020;368(6486):85-9.

52. Yang WS, SriRamaratnam R, Welsch ME, Shimada K, Skouta R, Viswanathan VS, et al. Regulation of ferroptotic cancer cell death by GPX4. Cell. 2014;156(1-2):317-31.

53. Stockwell BR, Jiang X. A Physiological Function for Ferroptosis in Tumor Suppression by the Immune System. Cell Metab. 2019;30(1):14-5.

SUPPORTING INFORMATION

Additional supporting information can be found online in the Supporting Information section at the end of this article.